Pergamon

Cement and Concrete Research 33 (2003) 299–304

CEMENT AND CONCRETE RESEARCH

# Study of alinite cement hydration by impedance spectroscopy

Young-Min Kim[a,b], Jong-Heun Lee[a], Seong-Hyeon Hong[a,*]

[a]School of Materials Science and Engineering, Seoul National University, Seoul 151-742, South Korea
[b]Division of Analysis and Measurement, Korea Basic Science Institute, Daejeon 305-333, South Korea

Received 1 May 2002; accepted 23 July 2002

## Abstract

Two types of alinite cements, Mg-alinite and Zn-alinite, were synthesized using the reagent grade chemicals. Their hydration behavior was compared with ordinary Portland cement (OPC) using impedance spectroscopy (IS) and $^{29}$Si nuclear magnetic resonance (NMR) spectroscopy. The bulk resistance in the IS spectra and the intensity ratio of the hydrous ($Q_1$ and $Q_2$) to anhydrous ($Q_0$) phases in the NMR spectra were estimated as the extent of hydration. The results obtained from both techniques were consistent each other. Mg-alinite had a comparable hydration rate to OPC and Zn-alinite exhibited faster hydration kinetics than Mg-alinite.

*Keywords:* Alinite; Portland cement; Hydration; Impedance spectroscopy (IS); Nuclear magnetic resonance (NMR)

## 1. Introduction

The reuse of industrial waste materials in cement manufacture has been established from the viewpoint of environmental protection and resource recycling [1–3]. Based on the use of waste products and low energy consumption, a new class of cement that is emerging is a chlorine bearing alinite [4–7]. The clinkering temperature for alinite was reported to be as low as 1000–1100 °C and its hydraulic properties were comparable or even superior to ordinary Portland cement (OPC) [4,8]. Also, alinite clinker has easy grindability compared to OPC resulting in a substantial energy saving for grinding [7]. Alinite has a comparable or even higher capacity of isomorphic substitution than alite (3–4%) [9–11]. The hydration products of alinite have a capability to fix heavy metals in the crystal lattice, which can be used to immobilize hazardous waste materials [5]. However, the likelihood of reinforcement corrosion by free chloride upon alinite hydration limits its applications, such as nonreinforced concrete products, marine structures, soil stabilization and oil-well cements [5,6,12–14]. In addition, little attention has been paid to the chemical synthesis of alinite and its hydration behavior.

In the past decade, impedance spectroscopy (IS) and nuclear magnetic resonance (NMR) spectroscopy have become promising techniques for probing cements and concretes. Cement paste is electrically conductive due to its interconnected pore network filled with an aqueous phase containing mobile ions such as $Na^+$, $K^+$ and $OH^-$ [11]. Since earlier work by McCarter et al. [15], the IS technique has been used to monitor the microstructural evolution, particularly the pore structure, in cement-based systems [15–22]. Several equivalent circuit models have been proposed to extract the physically meaningful parameters from the electrical responses of cement-based materials such as pore structure, pore size distribution and degree of hydration [23–25].

The main component of hydrated cement pastes is a calcium silicate hydrate (C–S–H) gel, which is a poorly crystalline material with a structure and composition that varies considerably [26]. NMR spectroscopy provides information about the local structure for both crystalline and amorphous materials [27] and has been used extensively to study the hydration of cements and related compounds [28–32]. $^{29}$Si and $^{27}$Al nuclei are commonly used to determine the local structural environment changes during the hydration of silicate or aluminate cements. In addition, the $^{1}$H cross polarization technique is especially useful for discriminating the signals from hydrous and anhydrous atomic environments. Thus, $^{29}$Si MAS NMR combined with

---

[*] Corresponding author. Tel.: +82-2-880-6273; fax: +82-2-883-8197.
*E-mail address:* shhong@plaza.snu.ac.kr (S.-H. Hong).

0008-8846/02/$ – see front matter © 2002 Elsevier Science Ltd. All rights reserved.
PII: S0008-8846(02)00944-4

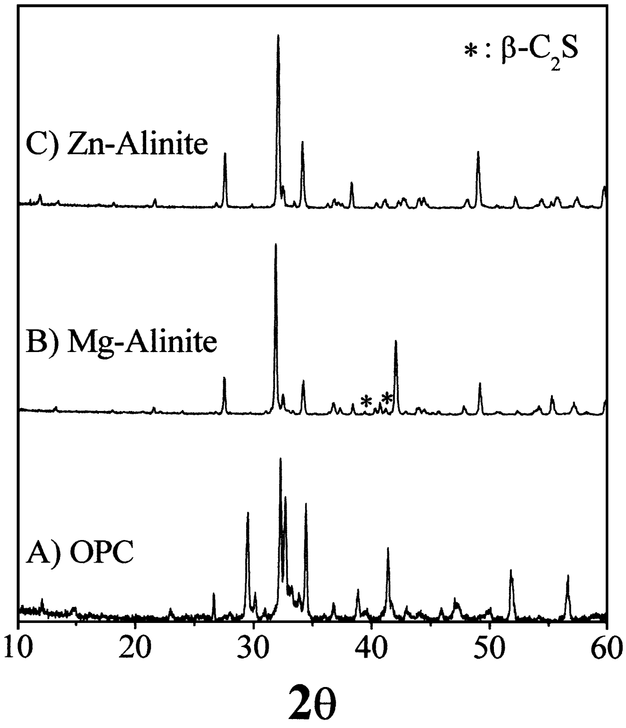

Fig. 1. XRD patterns of (A) OPC, (B) Mg-alinite and (C) Zn-alinite.

CP MAS NMR has the potential for quantitatively determining the extent of hydration in cement-based materials.

In this study, Mg- and Zn-substituted alinite clinkers were synthesized using reagent grade chemicals and their hydration behavior was investigated using IS, XRD and $^{29}Si$ MAS NMR. The hydration kinetics of alinite cements were compared with those of OPC.

## 2. Experimental procedures

Two types of alinite cements were synthesized based on the formula reported by Neubauer and Pollmann [12]; Mg-alinite ($Ca_{10}Mg_{0.8}\square_{0.2}[(SiO_4)_{3.4}(AlO_4)_{0.6}O_2Cl]$) and Zn-alinite ($Ca_{10}Zn_{0.8}\square_{0.2}[(SiO_4)_{3.4}(AlO_4)_{0.6}O_2Cl]$) (□: a lattice vacancy). The reagent grade chemicals, CaO, $SiO_2$, $Al_2O_3$, MgO, $CaCl_2$ and ZnO, were used as the starting materials. The raw materials were mixed in isopropyl alcohol, ball-milled for 24 h and then dried in an oven for 24 h. The dried mixtures were calcined at 1300 °C for 3 h. To minimize chlorine loss, a double crucible method was employed during calcination [12]. The hydration kinetics was compared with the commercially available OPC (LH Cement, Korea; 61.6% C = CaO, 21.2% S = $SiO_2$, 5.4% A = $Al_2O_3$, 3.2% F = $Fe_2O_3$, 3.6% M = MgO).

The specimens for the impedance measurement were prepared by hand mixing in an ambient atmosphere with a water to cement ratio of 0.4. The cement pastes were cast into the annular portion of the test fixtures similar to the one used by Christensen et al. [18] and the samples were stored in a sealed plastic container with a 100% relative humidity. The impedance measurements were performed using a SI 1260 impedance/gain-phase analyzer (Model No. SI 1260, Solartron, Farnborough, UK), and data acquisition was made over the frequency range from 100 Hz to 30 MHz at intervals of 10 points per decade.

The kinetics of the cement hydration was also investigated by XRD and $^{29}Si$ MAS NMR. For the measurements, the cast samples were demolded after a fixed curing time, and hydration was stopped by immersing the crushed samples in methanol for a week and then drying them in a $N_2$ atmosphere. The XRD and NMR measurements were then carried out on the dried cement pastes. $^{29}Si$ MAS NMR spectra were recorded at 79.50 MHz on Bruker DSX400 solid-state NMR spectrometer with a magnetic field of 9.4 T and a spin rate of 12–13 kHz.

## 3. Results and discussion

XRD patterns of OPC, Mg-alinite and Zn-alinite cements are shown in Fig. 1. OPC consisted of $C_3S$, $C_2S$, $C_3A$ and

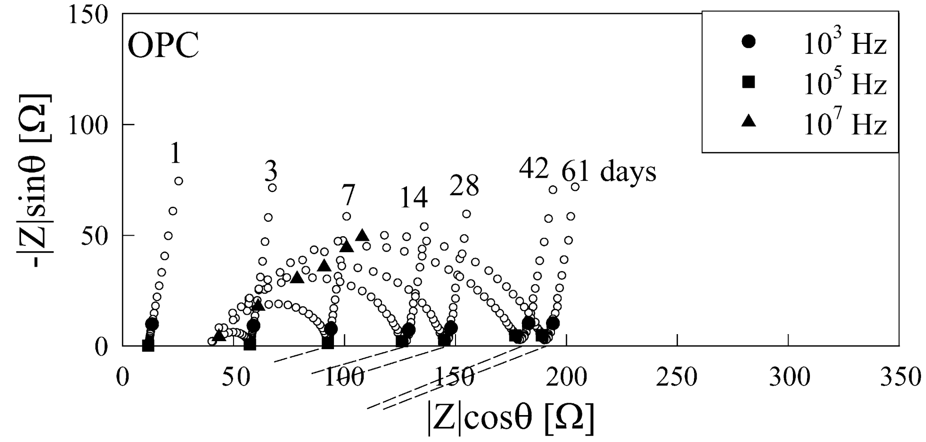

Fig. 2. Impedance spectra of OPC paste as a function of hydration time.

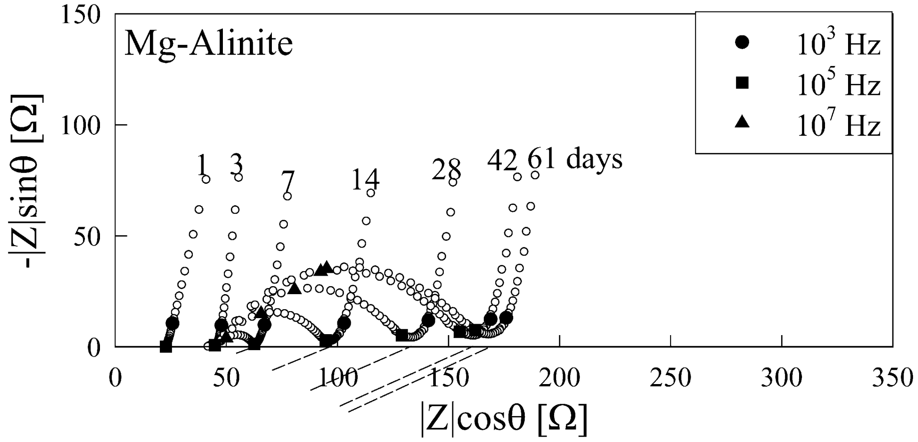

Fig. 3. Impedance spectra of Mg-alinite paste as a function of hydration time.

$C_4AF$, and the phase compositions were estimated to be 42.7%, 28.6%, 9.0% and 9.8%, respectively, according to Bogue's calculation [11]. It is generally agreed that MgO is essential for alinite formation [12,33]. Recently, Neubauer and Pollmann [12] reported that alinite does not have a fixed chemical composition and is more like a solid solution. Furthermore, it has been reported that alinite has a comparable or even higher capacity for isomorphic substitution than alite and $Mg^{2+}$ is known to be replaceable by $Ni^{2+}$, $Co^{2+}$, $Cu^{2+}$ and $Zn^{2+}$ [9]. Indeed, the XRD patterns showed that single-phase alinite was successfully obtained in both Mg- and Zn-substituted samples after sintering at 1300 °C for 3 h, with the exception of a minor amount of $C_2S$ in Mg-system (Fig. 1(B)). The specific surface area measured by BET was 1.0, 0.29 and 0.35 $m^2/g$ for OPC, Mg-alinite and Zn-alinite, respectively.

The Nyquist plots (imaginary versus real impedance) of OPC, Mg-alinite and Zn-alinite cement pastes are shown in Figs. 2–4, respectively. The frequency increased from right to left along the impedance curve and it is evident that there were two well-distinguished arcs except for the very early hydration. From the similar impedance spectra obtained in this study, the series $R_0-(R_1C_1)-(R_2C_2)$ model was proposed (Fig. 5) [16–18]. According to the equivalent circuit analysis, the low frequency arc (related with $R_2$ and $C_2$) represents the electrode–cement interface phenomenon and the high frequency arc (related with $R_1$ and $C_1$) is associated with bulk effects. Many impedance studies have reported an offset resistance ($R_0$) in cement hydration [15–21]. However, the explanation of the offset resistance is still controversial [18–21,25]. The $R_0$ values in OPC and Mg-alinite pastes increased continuously at early hydration until the appearance of a high frequency arc (Figs. 2 and 3) indicating that $R_0$ did not originate from the electrode but was bulk-related [18]. In this study, the bulk resistance of the cement pastes was determined from the intersection of low and high frequency arcs with the real impedance axis, which corresponds to the $R_0+R_1$ value in the equivalent circuit model shown in Fig. 5.

At early hydration (1 day), the high frequency arc was not well defined and only the low frequency arc was observed in OPC and Mg-alinite pastes. Zn-alinite paste exhibited both low and high frequency arcs even after 1-day hydration suggesting fast hydration compared to OPC and

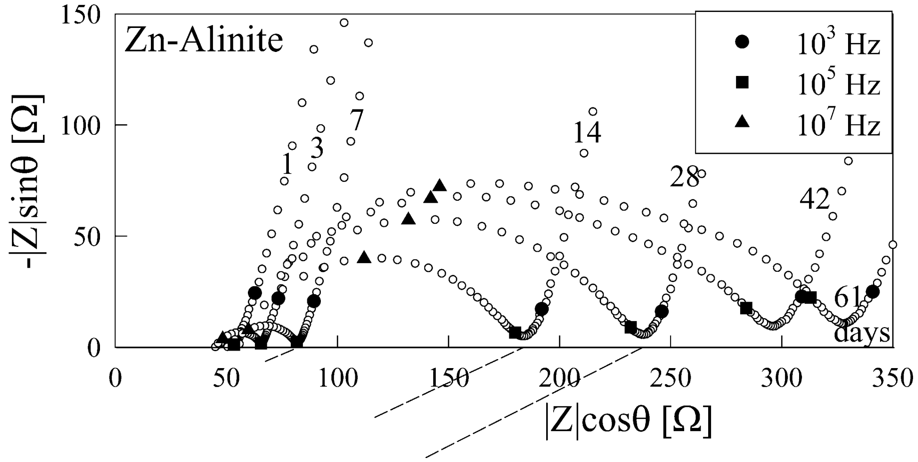

Fig. 4. Impedance spectra of Zn-alinite paste as a function of hydration time.

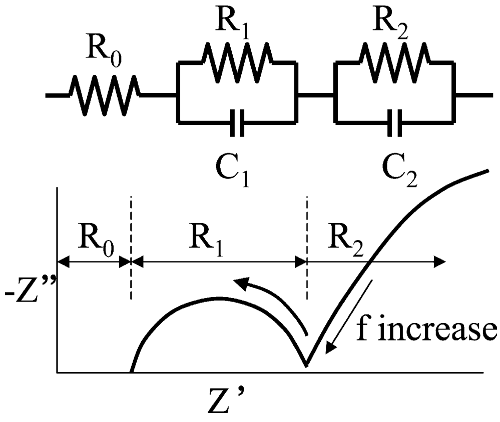

Fig. 5. Equivalent circuit model for the cement pastes.

Mg-alinite. As the hydration process progressed, the high frequency arcs appeared and the diameter of these arcs increased in all samples. However, the high frequency ends ($R_0$) were relatively unchanged if extrapolated to the real impedance axis after the high frequency arcs were formed. They were in the range of 40–45 Ω.

Fig. 6(A) shows the bulk resistance of the pastes as a function of the hydration time. The bulk resistances were observed to increase rapidly at earlier stage of hydration and change slowly at later stage in all the samples. OPC and Mg-alinite exhibited a similar bulk resistance with hydration time while Zn-alinite had a higher bulk resistance. The increase in the bulk resistance is associated with the hydration product formation and free water consumption. The conductivity (inverse of resistivity) of the cement pastes is expressed as

$$\sigma = \sigma_o \phi_{cap} \beta \qquad (1)$$

where $\sigma_o$ is the conductivity of the aqueous phase in the pores, $\phi_{cap}$ is the volume fraction of the capillary pores and $\beta$ is a connectivity factor. All three factors change with time for a given paste [21,34]. It is not appropriate to directly relate the bulk resistance to the degree of hydration in different cement systems without detailed information for each factor. However, a simple comparison based on the bulk resistance values indicated that Mg-alinite has a hydration rate comparable to OPC and Zn-alinite shows superior hydration kinetics compared to OPC. As observed in previous reports [15,18], the frequency at the intersection of low and high frequency arcs (cutoff frequency) varied with hydration time and type of cements (Fig. 6(B)). The frequency ranged from 10 to 200 kHz, and OPC, Mg-alinite and Zn-alinite pastes had similar frequencies for the same hydration time.

In addition, the centers of the high frequency arcs were depressed below the real axis (see Figs. 2–4). This non-Debye behavior was attributed to the spread of the relaxation time for the ions in the pore liquid [15] and was suggested to be related to the pore size distribution in the pastes [18,21]. The depression was more significant in Mg-alinite and Zn-alinite pastes implying a broad pore size distribution. Furthermore, the high frequency arcs of Zn-alinite pastes after 42- and 61-day hydration appears to have two contributions, which might reflect that Zn-alinite at later stage of hydration becomes electrically more heterogeneous compared to OPC and Mg-alinite. As an alternative explanation proposed by Ford et al. [35] in the aged OPC/silica fume specimen with steel electrode, one of the two contributions (low frequency side) could be assigned to the imperfect electrode contact due to the preferential drying and/or shrinkage cracking. Thus, the low frequency contribution in Zn-alinite was excluded by the deconvolution analysis and the results were inserted using the filled circle in Fig. 6(A). The relatively abrupt increase in the $R_0 + R_1$ values after 42-day hydration was reduced as marked arrows and smoothly connected with other data although overall

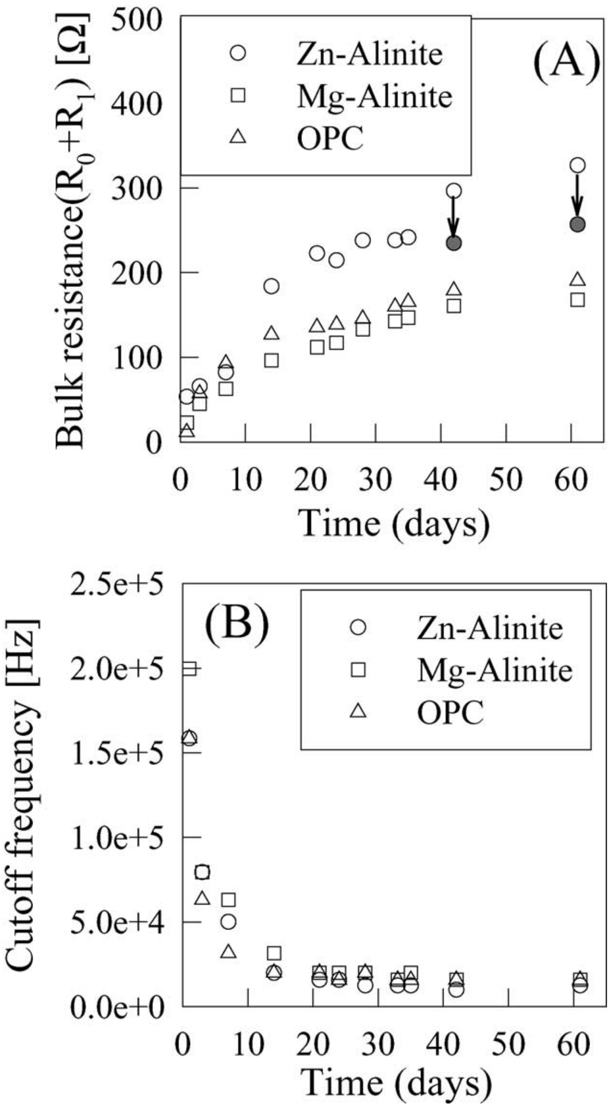

Fig. 6. (A) Bulk resistance and (B) cut-off frequency as a function of hydration time in OPC, Mg-alinite and Zn-alinite pastes. The inserted filled circles were the deconvoluted values by removing the contribution from the imperfect electrode as proposed by Ford et al. [35].

tendency in Zn-alinite was not changed. However, further studies are required to identify the reasons and confirm the above interpretations.

The degree of hydration in OPC, Mg-alinite and Zn-alinite was further investigated by both XRD and $^{29}$Si MAS NMR for the comparison with the results from IS. The XRD patterns of the pastes hydrated for 28 days are shown in Fig. 7. The main hydration products were C–S–H gels and $Ca(OH)_2$ in OPC, Mg- and Zn-alinite, and unhydrated cements still remained in all the pastes. The weak intensity peaks of the Friedel's salt-like phase were also observed in the alinite pastes. The composition of the Friedel's salt-like phase has been proposed to be $C_3A{\cdot}CaY_2{\cdot}10H_2O$ ($Y = 1/2CO_3^{2-}$, $(OH)^-$, $Cl^-$) [12]. The peak intensity of the unreacted alinite in Zn-alinite paste was weaker than that in Mg-alinite indicating a fast hydration rate in Zn-alinite. However, it was difficult to compare the degree of hydration with OPC directly.

The $^{29}$Si MAS NMR spectra for the pastes hydrated for 28 days are shown in Fig. 8. The hydrates of OPC exhibited two broad peaks at − 71.5 and 79 ppm and a weak shoulder at − 84 ppm (Fig. 8(A)). The chemical shift of − 71.5 ppm ($Q_0$) was assigned to unhydrated OPC and both − 79 ($Q_1$) and − 84 ($Q_2$) ppm peaks were to the hydrates because they were cross-polarized. OPC mainly consisted of $C_3S$ and $C_2S$. $C_3S$ is known to have seven NMR peaks between − 68.9 and − 74.5 ppm, and $C_2S$ has one peak at about − 71 ppm [31]. However, the $Q_0$ peak in this spectrum was less well resolved probably due to the presence of impurities in OPC. The absence of $Q_3$ and $Q_4$ in the hydrates of OPC indicated that the predominant species in the C–S–H gels were dimers. In the hydrates of Mg- and Zn-alinites, two $Q_0$ peaks were observed at − 71 and − 75 ppm. It was reported that alinite has one unique Si position in an isolated tetrahedron [36]. Therefore, the peak at − 75 ppm could be assigned to alinite and the weak peak at − 71 ppm could be assigned to $C_2S$ although $C_2S$ was not well identified in the XRD patterns. Similar hydration products ($Q_1$ and $Q_2$) were detected in the alinite pastes.

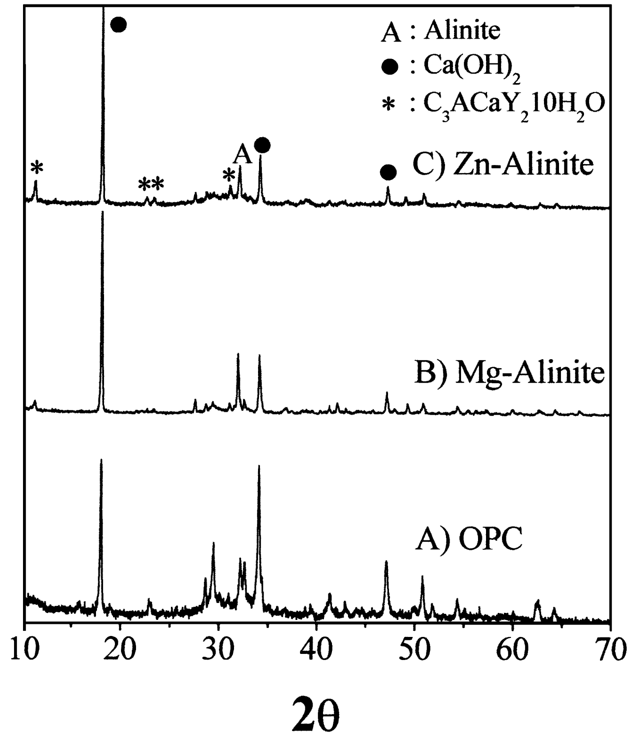

Fig. 7. XRD patterns of the hydrated pastes cured for 28 days: (A) OPC, (B) Mg-alinite and (C) Zn-alinite.

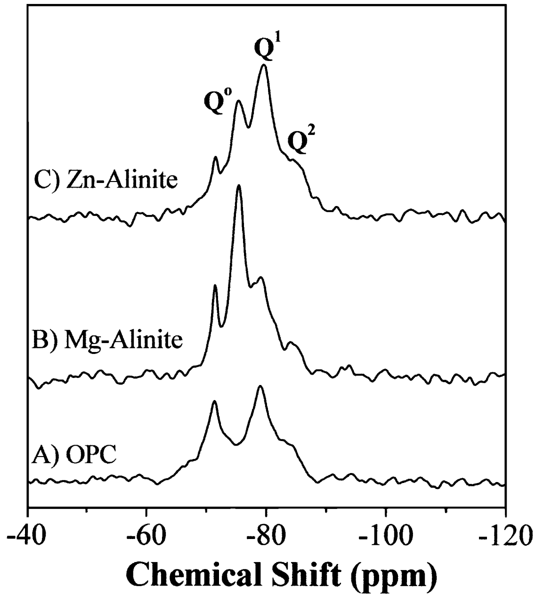

Fig. 8. $^{29}$Si MAS NMR spectra of the hydrated pastes cured for 28 days: (A) OPC, (B) Mg-alinite and (C) Zn alinite.

The degree of hydration was estimated by the intensity ratio of the NMR peaks, $\{(Q_1 + Q_2)/(Q_0 + Q_1 + Q_2)\} \times 100$ [32]. It was 47%, 41% and 61% after 14-day hydration for OPC, Mg-alinite and Zn-alinite, respectively, and changed to 63%, 45% and 66% after 28 days, correspondingly. The hydration kinetics of Zn-alinite was much faster than that of Mg-alinite with OPC being somewhere in between. These results generally agree with those obtained from IS. However, the details were slightly different such that Mg-alinite was close OPC after 14-day hydration and Zn-alinite was close to OPC after 28 days by NMR although Mg-alinite was always like OPC by IS. Additional information using other techniques such as conduction calorimeter will help to explain the differences and provide the better representative values to describe the hydration kinetics. In addition, calcium chloride is known to accelerate the hydration of Portland cement [11]. The $Cl^-$ ion exsolution from the alinite pastes was significant, but the $Cl^-$ concentrations in Mg- and Zn-alinite were approximately same, that is, 1200 ppm (~ 0.034 mol/l) after 14 days [37]. Thus, the effect of free chlorine was not enough to explain the different hydration kinetics in Mg- and Zn-alinites.

## 4. Summary

The hydration of Mg-alinite and Zn-alinite cements was investigated using IS and $^{29}$Si MAS NMR spectroscopy. In impedance spectra, the bulk resistance of Zn-alinite cement was substantially larger than that of OPC, while Mg-alinite cement was similar to OPC. XRD and NMR further confirmed the fast hydration of Zn-alinite cement.

## References

[1] B. Dawson, Emerging technologies for utilizing waste in cement production, World Cem. 23 (12) (1992) 22–24.

[2] H. de Ladebat, D. Lemarchand, Waste management, World Cem. 31 (3) (2000) 70–78.

[3] J. Forgey, Reusing waste materials, World Cem. 31 (5) (2000) 122–127.

[4] P.D. Vaidyanathan, P.C. Kapur, B.N. Singh, Production and properties of alinite cements from steel plant wastes, Cem. Concr. Res. 20 (1) (1990) 15–24.

[5] H. Motzet, J. Neubauer, H. Pollmann, Alinite-cement made from waste incineration residues—from basic research to application, Proceedings of the 16th International Conference on Cement Microscopy, Richmond, VA, 1994, pp. 210–229.

[6] H. Poellmann, J. Neubauer, H. Motzet, The usage of industrial waste materials for the production of special cements and binders, in: S. Diamond, S. Mindess, F.P. Glasser, L.W. Roberts, J.P. Skalny, L.D. Wakeley (Eds.), Microstructure of Cement Based Systems/Binding and Interfaces in Cementitious Materials, Materials Research Society, Pittsburgh, PA, 1995, pp. 169–178.

[7] F.W. Locher, Low energy clinker, 8th International Congress on the Chemistry of Cement, Vol. I, Brazil, 1986, pp. 57–67.

[8] F. Massazza, C. Gilioli, Contribution to the alinite knowledge, Il Cemento 2 (1983) 101–106.

[9] F.V. Lampe, K.H. Jost, B. Wallis, P. Leibnitz, Synthesis, crystal structure and properties of a new calcium-magnesium-monosilicate-chloride, $Ca_8Mg[(SiO_4)_4Cl_2]$, Cem. Concr. Res. 16 (5) (1986) 624–632.

[10] F. von Lampe, Isomorphe Substititionen bei Alinit, Silikattechnik 39 (6) (1988) 194–198.

[11] H.F.W. Taylor, Cement Chemistry, 2nd ed., Thomas Telford, London, UK, 1997.

[12] J. Neubauer, H. Pollmann, Alinite-chemical composition, solid solution and hydration behaviour, Cem. Concr. Res. 24 (8) (1994) 1413–1422.

[13] J. Bensted, A discussion of the paper 'Alinite-Chemical Composition, Solid Solution and Hydration Behavior' by J. Neubauer and H. Pollmann, Cem. Concr. Res. 25 (8) (1995) 1806–1807.

[14] M. Motzet, H. Pollmann, J. Neubauer, A reply to a discussion by John Bensted of the paper 'Alinite-Chemical Composition, Solid Solution and Hydration Behavior', Cem. Concr. Res. 25 (8) (1995) 1808–1810.

[15] W.J. McCarter, S. Garvin, N. Bouzid, Impedance measurements on cement paste, J. Mater. Sci. Lett. 7 (10) (1988) 1056–1057.

[16] W.J. McCarter, R. Brousseau, The A.C. response of hardened cement paste, Cem. Concr. Res. 20 (1990) 891–900.

[17] C.A. Scuderi, T.O. Mason, H.M. Jennings, Impedance spectra of hydrating cement pastes, J. Mater. Sci. 26 (1991) 349–353.

[18] B.J. Christensen, T.O. Mason, H.M. Jennings, Influence of silica fume on the early hydration of Portland cements using impedance spectroscopy, J. Am. Ceram. Soc. 75 (4) (1992) 939–945.

[19] P. Gu, P. Xie, J.J. Beaudoin, R. Brousseau, A.C. impedance spectroscopy: I. A new equivalent circuit model for hydrated Portland cement paste, Cem. Concr. Res. 22 (1992) 833–840.

[20] P. Gu, Z. Xu, P. Xie, J.J. Beaudoin, Application of A.C. impedance techniques in studies of porous cementitious materials: I. Influence of solid phase and pore solution on high frequency resistance, Cem. Concr. Res. 23 (1993) 531–540.

[21] B.J. Christensen, R.T. Coverdale, R.A. Olson, S.J. Ford, E.J. Garboczi, H.M. Jennings, T.O. Mason, Impedance spectroscopy of hydrating cement-based materials: measurement, interpretation, and application, J. Am. Ceram. Soc. 77 (11) (1994) 2789–2804.

[22] G. Dotelli, C.M. Mari, The evolution of cement paste hydration process by impedance spectroscopy, Mater. Sci. Eng. A 303 (2001) 54–59.

[23] K. Brantervik, G.A. Niklasson, Circuit models for cement based materials obtained from impedance spectroscopy, Cem. Concr. Res. 21 (1991) 496–508.

[24] D.E. Macphee, D.C. Sinclair, S.L. Cormack, Development of an equivalent circuit model for cement paste from microstructural considerations, J. Am. Ceram. Soc. 80 (11) (1997) 2876–2884.

[25] G. Song, Equivalent circuit model for AC electrochemical impedance spectroscopy of concrete, Cem. Concr. Res. 30 (2000) 1723–1730.

[26] D. Viehland, J.-F. Li, L.-J. Yuan, Z. Xu, Mesostructure of calcium silicate hydrate (C–S–H) gels in Portland cement paste: short-range ordering, nanocrystallinity, and local compositional order, J. Am. Ceram. Soc. 79 (7) (1996) 1731–1744.

[27] G.L. Turner, R.J. Kirkpatrick, S.H. Risbud, E. Oldfield, Multinuclear magic-angle sample-spinning nuclear magnetic resonance spectroscopic studies of crystalline and amorphous ceramic materials, J. Am. Ceram. Soc. Bull. 66 (4) (1987) 656–663.

[28] J. Hjorth, J. Skibsted, H.J. Jakpbsen, $^{29}$Si MAS NMR studies of Portland cement components and effects of microsilica on the hydration reaction, Cem. Concr. Res. 18 (1988) 789–798.

[29] X. Cong, R.J. Kirkpatrick, Hydration of calcium aluminate cements: a solid-state $^{27}$Al NMR study, J. Am. Ceram. Soc. 76 (2) (1993) 409–416.

[30] G. Sun, A.R. Brough, J.F. Young, $^{29}$Si NMR study of the hydration of $Ca_3SiO_5$ and $\beta$-$Ca_2SiO_4$ in the presence of silica fume, J. Am. Ceram. Soc. 82 (11) (1999) 3225–3230.

[31] R.J. Kirkpatrick, X.-D. Cong, An introduction to $^{27}$Al and $^{29}$Si NMR spectroscopy of cements and concretes, in: P. Colombet, A.-R. Grimmer (Eds.), Application of NMR Spectroscopy to Cement Science, Gordon and Breach Science Publisher, Singapore, 1994, pp. 55–75.

[32] S.-H. Hong, J.F. Young, Hydration kinetics and phase stability of dicalcium silicate synthesized by the pechini process, J. Am. Ceram. Soc. 82 (7) (1999) 1681–1686.

[33] Ch. Ftikos, Th. Philippou, J. Marinos, A study of the effect of some factors influencing alinite clinker formation, Cem. Concr. Res. 23 (6) (1993) 1268–1272.

[34] E.J. Garboczi, Permeability, diffusivity, and microstructural parameters: a critical review, Cem. Concr. Res. 20 (1990) 591–601.

[35] S.J. Ford, J.D. Shane, T.O. Mason, Assignment of features in impedance spectra of the cement-paste/steel system, Cem. Concr. Res. 28 (12) (1998) 1737–1751.

[36] V.V. Ilyukhin, N.N. Nevsky, M.J. Bickbau, R.A. Howie, Crystal structure of alinite, Nature 269 (1977) 397–398.

[37] Y.-M. Kim, S.-H. Hong, H.-M. Park, Isomorphic substitution and hydration behavior of alinite cement, submitted to J. Eur. Ceram. Soc.